Biochimica et Biophysica Acta, 391 (1975) 361—381

BBA 67500

PURIFICATION AND CHARACTERIZATION OF *ASPERGILLUS NIGER* EXO-1,4-GLUCOSIDASE

IRWIN M. FREEDBERG*, YEHUDA LEVIN[a], CYRIL M. KAY[b], WILLIAM D. McCUBBIN[b] and EPHRAIM KATCHALSKI-KATZIR[a]

[a]*Department of Biophysics, Weizmann Institute of Science, Rehovot (Israel) and* [b]*Department of Biochemistry, University of Alberta, Edmonton (Canada)*

(Received July 25th, 1974)
(Revised manuscript received February 24th, 1975)

Summary

A specific exo-1,4-glucosidase (1,4-α-D-glucan glucohydrolase, EC 3.2.1.3) from *Aspergillus niger* has been partially purified and subsequently characterized by biochemical, physico-chemical and optical methods. Molecular sieve chromatography yields an enzyme with maximal activity at pH 4.2—4.5 close to its isoelectric point. Reduction and carboxymethylation leads to complete loss of activity and O-acetylation of 3 of the 13 tyrosine residues results in loss of 20% of the activity. Sodium dodecylsulfate-polyacrylamide gel electrophoresis indicates that the native enzyme consists of two major components of molecular weights 63 000 and 57 500, respectively. Small amounts of dissociated material of molecular weight 28 000—30 000 and 16 000 as well as aggregates of the order of 100 000 are also present to the extent of 2—5% of the total protein. Following reduction and carboxymethylation under forcing conditions, the bands around 60 000 diminish and the 28 000—30 000, 16 000 and aggregate bands are dominant. Sedimentation-diffusion studies indicate that the native molecule has an apparent molecular weight of 62 000. Sedimentation equilibrium measurements extended to a concentration range below that attainable by the sedimentation-diffusion, suggest that the enzyme is an oligomeric system formed from 30 000, and possibly also 16 000 subunits.

At the pH of maximal enzymatic activity (4.2) Moffit-Yang plots constructed from optical rotatory dispersion (ORD) measurements between 500 and 300 nm linearize with a λ_0 of 205 nm and indicate a b_0 value of −169°. A negative Cotton occurs in ORD at 228 nm and shifts toward higher wavelengths (233 nm) with elevation of temperature. The necessity to linearize the Moffitt

* Present address: Department of Dermatology, Beth Israel Hospital, Harvard Medical School, Boston, Mass, U.S.A.

plots with a λ_0 of 205 nm as well as the position of the Cotton minimum at a wavelength lower than 233 nm may reflect the large amount of carbohydrate, (15%), in the native enzyme, and its possible interaction with the protein moiety.

Circular dichroism (CD) has been measured in both near and far ultraviolet ranges. Negative bands are observed at 218 and 209 nm with ellipticity values of −8200 and −8000 degree · $dmol^{-1}$ · cm^{-2}, respectively. A broad band of negative ellipticity occurs between 285 and 268 nm with minima of 30–40 degree · $dmol^{-1}$ · cm^{-2} at 285, 278, and 275 nm. O-Acetylation of the enzyme as well as exposure to alkaline pH indicates that this band arises from asymmetrical interactions involving tyrosine residues, although tryptophan contributions may also be involved. A positive band at 258 nm of 10–12 degree · $dmol^{-1}$ · cm^{-2} is found in the native protein and is attributable to both tyrosine and cystine residues in asymmetric environments, since it undergoes a red shift at pH values above 9.4, while becoming less negative, as well as a substantial decrease following reduction and carboxymethylation. Far ultraviolet CD studies of the enzyme indicate a small but significant decrease in secondary structure when the enzyme reacts with synthetic substrate or inhibitor.

Comparison of the spectra generated with those published for model polypeptides and proteins whose crystallographic structure is known suggests that the native molecule of exo-1,4-glucosidase contains 15–25% α-helix in addition to β structure and disordered configuration. The presence of all three conformational forms in the native protein was verified by infrared studies on ^2H_2O solutions and films prepared from the enzyme.

Introduction

Enzymes have been isolated from extracts of bacterial, fungal and animal origin which hydrolyze starch almost completely to D-glucose [1]. Characterization of these exo-1,4-glucosidases (glycan hydrolases, EC 3.2.1.3) has revealed them to be glycoproteins of molecular weight between 50 000 and 100 000 [2] with hydrolytic activity predominantly directed toward α-D 1,4 linkages, although some α-D 1,6 activity is also present [3]. Evidence for the existence of two closely related forms of the enzyme in extracts of *Aspergillus niger* has been presented by several authors [1,4,5].

The studies reported in this communication were aimed at the purification, biochemical characterization and physico-chemical study of the exo-1,4-glucosidase from *A. niger*. The studies were stimulated by our ultimate aim: the production of an active insoluble derivative of the enzyme, an approach which has been undertaken by several other groups interested in such enzymes [6,7]. Utilizing the techniques of optical rotatory dispersion, circular dichroism and infrared spectroscopy, we have been able to obtain for the first time data concerning the secondary and tertiary structure of this molecule. Sedimentation equilibrium and sodium dodecylsulfate-polyacrylamide gel electrophoretic data on the native and reduced carboxymethylated material indicate the existence of a multichain enzyme whose conformation can be explained on the basis of a mixture of α, β and disordered areas of polypeptide chain, influenced perhaps by interaction with the carbohydrate side chains.

Materials and Methods

Partially purified amyloglucosidase was obtained as a gift from Miles Laboratories, Elkhart, Indiana (Diazyme) and was subsequently purified to electrophoretic homogeneity by chromatography on acrylamide columns. Chromatographic procedures were carried out at room temperature. Elution peaks were identified by continuous monitoring of the absorbance at 280 nm, and absorbance of the specific fractions was determined in a Zeiss PMQ II spectrophotometer. Protein concentrations were determined by the procedure of Lowry et al. [8] or by calculation from the absorptivity coefficient of 280 nm ($\epsilon^{1\%}_{1\,cm}$ = 13.6). Total nitrogen was determined by the Kjeldahl reaction [9], and carbohydrate by the phenolsulfuric acid procedure [10] using D-glucose as a standard. Ultraviolet absorption spectra were recorded on a Cary 14 spectrophotometer following appropriate dilution in either neutral buffers or 0.1 M NaOH. Enzymatic activity was determined using the synthetic substrate *p*-nitrophenyl-α-D-glucopyranoside and a modification of the technique of Sternberg [11]. One unit of enzymic activity was defined as that amount of enzyme which hydrolyzed 1 μmol of substrate in 15 min at 60°C under the conditions employed. During purification additional assays were performed with the natural substrate (soluble starch solution). Liberated glucose was quantitated by the glucose oxidase method (Glucostat, Worthington Biochemical).

Acid hydrolyses and amino acid analyses were performed according to the technique of Moore and Stein [12].

Acrylamide gel disc electrophoresis was performed at pH 8.6 following the procedure of Davis [13]. Preparative electrophoresis in acrylamide was undertaken in a Shandon apparatus using the technique suggested by the manufacturers (Shandon Scientific, Co. Ltd., 65 Pound Lake, Dondon, N.W. 10). Analytical gel electrofocusing was performed in the presence of ampholyte ("Ampholine") and the enzyme as described by Wrigley [14] (Method B). Preparative electrofocusing was done with an LKB apparatus using the technique described by Haglund [15]. Sodium dodecylsulfate-polyacrylamide gel electrophoresis experiments were performed on 10% polyacrylamide gels containing 0.1% sodium dodecylsulfate as outlined by Weber et al. [16]. Samples were prepared in 1–2% sodium dodecylsulfate solution containing 1 mM dithiothreitol by heating in a boiling water bath for 1–5 min.

Sulfhydryl content of the protein was determined according to Ellman [17]. Amino-terminal residues were identified by the cyanate method of Stark and Smyth [18], Sanger's dinitrophenol method [19], Edman's phenylthiohydantoin method [20], digestion by leucine amino peptidase [21], as well as by the dansyl procedure as outlined by Woods and Wang [22] using an excess of 1-dimethyl aminonaphthalene-5-sulfonyl chloride. O-Acetylation of tyrosine residues was carried out according to the procedure of Riordan et al. [23] using a 200-fold excess of acetylimidazole. Tryptophan and tyrosine were determined spectrophotometrically according to Edelhoch [24]. Reduced carboxymethylated enzyme was prepared according to the procedure of Crestfield et al. [25].

Circular dichroism and optical rotatory dispersion were measured on a

Cary 6001 recording spectropolarimeter calibrated with d-10 camphor sulfonic acid. 1-cm quartz cells were used for readings from 600 to 250 nm and cells of 0.2—2-mm path length were used for readings in the 250- and 185-nm range. All measurements were obtained with an absorbance of less than 2 and at 29° C unless otherwise noted. Optical rotatory dispersion data are presented as reduced mean residue rotations (m') and circular dichroism data are presented as mean residue ellipticity (θ) in degrees · $dmol^{-1}$ · cm^{-2}. The mean residue weight of 115 was calculated from the amino acid composition of the enzyme. Signal to noise ratios at band maxima were often as high as 25 : 1 and were never lower than 10 : 1. The errors in ellipticity value were estimated to be less than 10% in the aromatic region, approx. 3% in the 210—225-nm range and 7% at 192—195 nm.

A Spinco Model E analytic ultracentrifuge equipped with Schlieren optics was used for sedimentation and diffusion studies. Sedimentation velocities were measured at or near 20° C and were corrected according to the usual relationships for solvent density and viscosity. Apparent diffusion coefficients were determined according to a modification of the boundary spreading technique of Pickels [26] in which a synthetic boundary cell was used. The maximum ordinate-area method of Fujita [27] was utilized for calculations and all data were standarized to water at 20° C. The apparent molecular weight was estimated by substitution of the intrinsic values of S and D in the Svedberg equation [28], $M = RTs/(1 - \bar{v}p)D$, in which all symbols have their usual significance.

Molecular weight studies employing the technique of sedimentation equilibrium were carried out at 20° C in a Beckman Spinco Model E ultracentrifuge equipped with photoelectric scanner, multiplex accessory, high intensity light source and Rayleigh interference optical system. Double-sector, charcoal-filled epon cells with wide-aperture window holders were used. Conventional sedimentation equilibrium experiments were performed according to the methodology of Chervenka [29], using rotor speeds of 9000—15 000 rev./min.

Infrared absorption spectra were generated in a Beckman IR-7 spectrophotometer calibrated with atmospheric water vapor bands. Samples were studied in cells with CaF_2 windows following extensive dialysis against ^2H_2O or on films prepared on NaCl plates and dried over P_2O_5. (We are indebted to Dr S. Pinchus of the Organic Chemistry Department of the Weizmann Institute for performing the infrared measurements.

Results and Discussion

Separation and purification

Lineback et al. [5] utilized DEAE-cellulose chromatography with a discontinuous citrate/phosphate buffer system to purify fungal exo-1,4-glucosidase. In our laboratory the technique did yield enzymic activities eluting from the column at pH 6.0 and 4.0 but the amino acid composition (Table I) and molecular kinetic properties of the two fractions as measured by sedimentation and diffusion were identical. The chromatographic elution pattern itself was not reproducible from batch to batch of crude enzyme and, although it elimi nated an inactive chromagenic contaminant from the preparations, this te

nique did not result in significant purification. Barton and coworkers [30] have pointed out that the elution characteristics of amyloglucosidase depend upon the medium in which the *Aspergillus* is grown. When the medium is glucose/NH_4Cl, the concentration of the enzyme eluting at pH 6 is markedly decreased and this seemed to be the case in the material which we studied.

A number of other preparative techniques were subsequently studied but eliminated for a variety of reasons. Dialysis effectively eliminated chromogenic contaminants but it resulted in leakage from the bags ascribed to the presence of cellulase contaminants. A 40–60% $(NH_4)_2SO_4$ cut also eliminated the chromogenic contaminant but did not result in significant purification. Analytic electrophoresis yielded two active forms of the enzyme but we were unable to separate these with the preparative electrophoretic equipment available to us.

Since exo-1,4-glucosidase is a glycoprotein we attempted to use insoluble concanavalin A in an affinity chromatographic column. No increase in specific activity resulted, apparently due to the fact that the non-active components of the crude enzyme mixture were also glycoproteins. Analytic electrofocusing of the enzyme indicated two major protein species with isoelectric points of pH 3.2 and 4.0 with the pH 3.2 species in higher concentration. Preparative isofocusing could not be used, however, since the major component precipitated in the focusing column.

The preparative procedure which we were able to use is illustrated in Figs 1 and 2. It depends upon molecular sieve chromatography on either Sephadex G-100 or Biogel P-150. In both cases the protein could be efficiently and rapidly separated from the major chromogenic contaminant with over 90% recovery of enzymic activity. In the case of Sephadex, variation in the sugar content of the eluted enzyme as well as erratic elution rates were commonly seen and these have been attributed to digest of the macromolecular structure of Sephadex itself by the enzyme. The Biogel method, therefore, has been used

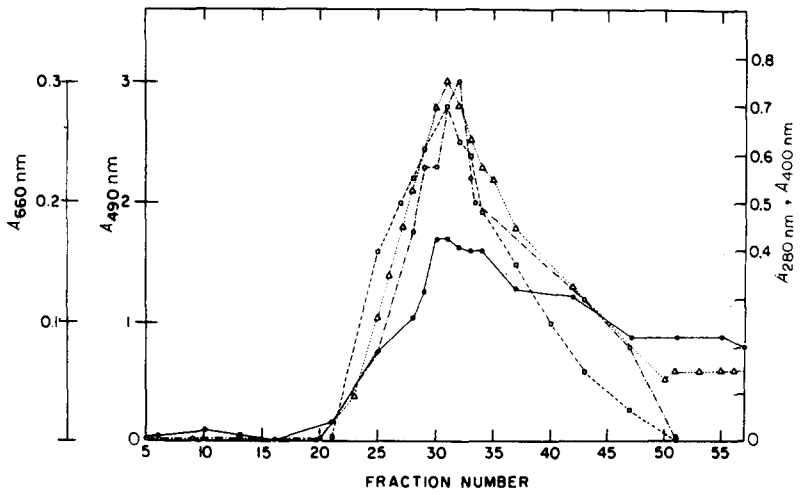

Fig. 1. Purification of Diazyme L-30 on Sephadex G-100 column. □- - - - -□, absorbance at 280 nm; △· · · · ·△, absorbance at 660 nm (protein content, Lowry et al. [8]); ○— · — ·○, absorbance at 400 nm (activity); ●———●, absorbance at 490 nm (sugar determined by the phenol test).

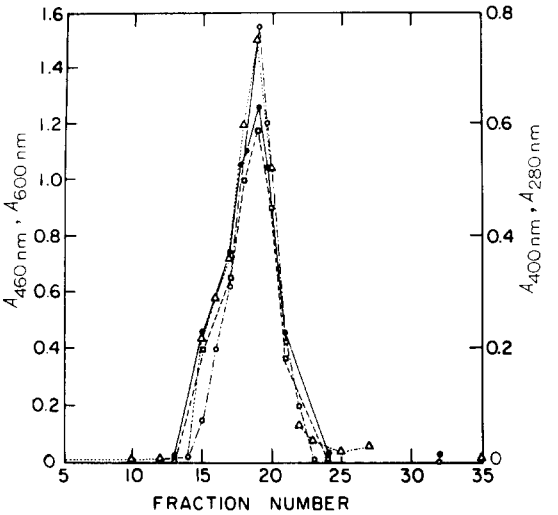

Fig. 2. Purification of Diazyme L-30 on a Biogel P-150 column. △- - - - -△, absorbance at 280 nm. ○— · — ·○, absorbance at 660 nm (protein content, Lowry et al. [8]); ●————●, absorbance at 400 nm (activity); □- - - - -□, absorbance at 490 nm (sugar content).

in all our subsequent studies since the minor bands evident on acrylamide electrophoresis or analytical electrofocusing are not components of the major Biogel peak and the method itself is readily reproducible. The method may be scaled up to any enzyme level which is desirable and is rapid, efficient and reproducible.

Biochemical characterization of exo-1,4-glucosidase

The amino acid composition of the purified enzyme is given in Table I (column C). The cystine content was determined using performic acid oxidized and reduced carboxymethylated exo-1,4-glucosidase. Six half-cystine residues per mol were found. No free SH groups could be detected using Ellman's procedure [17]. The nature of the N-terminal amino acid(s) was investigated by several techniques (see Materials and Methods). No free N-terminal amino acid residue could be detected. The tyrosine and tryptophan contents were determined by the Edelhoch technique [24]. There were 13 tyrosine and 14 tryptophan residues per mol. Spectrophotometric titration (Fig. 3) indicated that no clear differentiation could be made between buried and natural tyrosines in the molecule. The fluorescent quantum yield of the tryptophans at an excitation wavelength of 280 nm and an emission wavelength of 350 nm was 12%.

Atomic absorption studies revealed no significant concentration of heavy metals associated with the purified enzyme, a finding which was confirmed by the lack of effect on enzymatic activity of ethylenediaminetetracetic acid up to a concentration of 10^{-2} M. Reduction and carboxymethylation led to total loss of enzyme activity while O-acetylation of 3 of the 13 tyrosine residues was associated with loss of only 20% of the enzyme activity.

The pH dependence of the rates of hydrolysis and stability of the enzyme are shown in Fig. 4. The optimal pH of activity (pH 4.2—4.5) with *p*-nitro-

TABLE I

AMINO ACID COMPOSITION OF PERFORMIC ACID OXIDIZED EXO-1,4-GLUCOSIDASE PREPARATIONS

Results expressed in μmol/100 mg enzyme preparation.

	Preparation A	Preparation B	Preparation C
Lysine	12.0	9.3	9.1
Histidine	4.3	4.4	3.1
Arginine	15.5	13.5	16.6
Cysteic acid	9.2	7.3	12.7
Aspartic acid	65.3	53.6	58.0
Threonine	63.2	48.7	52.0
Serine	76.0	58.8	56.0
Glutamic acid	39.8	34.0	35.0
Proline	18.3	20.4	—
Glycine	44.2	35.7	38.0
Alanine	61.0	49.6	47.0
Valine	32.0	27.7	31
Methionine	—	—	—
Isoleucine	14.7	12.0	18
Leucine	40.4	32.8	36
Tyrosine	18.1	4.9	—
Phenylalanine	18.6	15.1	13

Preparations A and B are the fractions eluting from DEAE at pH 6.0 and pH 4.0, respectively, obtained from the enzyme preparation 20-2698. Preparation C is the fraction eluting from Biogel.

phenyl-α-D-glucopyranoside as substrate was close to the isoelectric point of the enzyme as determined by electrofocusing. The enzyme remained stable, however, up to a pH of 10.0 at which point a rapid irreversible loss of enzymatic activity occurred. As noted below, conformational studies based upon circular dichroism and optical rotatory dispersion measurements indicated an irreversible conformational change associated with loss of α-helix and development of the random orientation at this same pH. Temperature stability studies indicated preservation of the α-helix up to the same temperature.

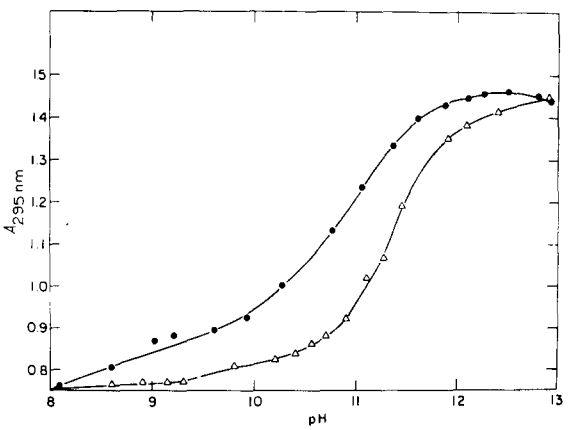

Fig. 3. Spectrophotometric titration of tyrosines in exo-1,4-glucosidase, 1.5 mg/ml in 0.1 M KCl, temperature 25° C. △———△, direct titration; ●———●, back titration.

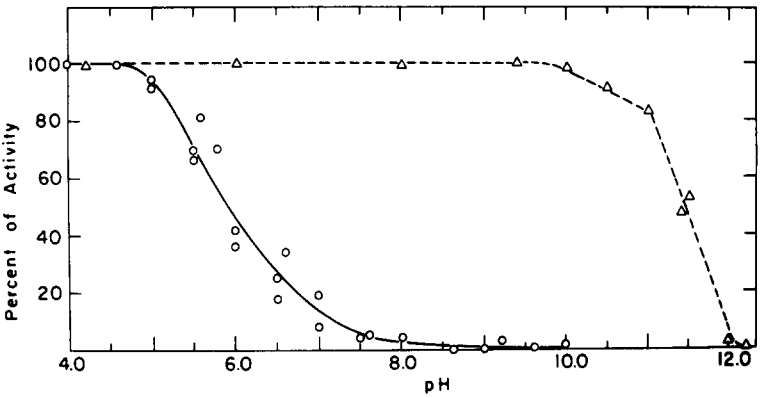

Fig. 4. pH vs activity and pH vs stability curves. For the pH vs stability determinations the enzyme was incubated at room temperature for 1 h at the pH indicated; aliquots were removed and assayed at pH 4.2. Buffers: pH 3.4—6.0, 0.1 M acetic acid/sodium acetate; pH 6.0—8.0, 0.1 M phosphate; pH 8.0—9.0, 0.1 M Tris · HCl; pH 9.0—12.2, 0.1 M glycine/NaCl. ○———○, pH vs activity curve; △- - - - -△, pH vs stability curve.

The Lineweaver and Burk plot of the kinetics of exo-1,4-glucosidase catalyzed hydrolysis of *p*-nitrophenyl-α-D-glycopyranoside is shown in Fig. 5. A value of $3 \cdot 10^{-3}$ M was estimated for the Michaelis constant (K_m). The K_m of the enzyme using its natural substrate, starch, has not been determined. Enzymic activity could be inhibited with gluconolactone and a value of $8 \cdot 10^{-3}$ M was obtained for the inhibition constant (K_i) from kinetic studies. Fluorescence quenching measurements [31] yielded a dissociation constant of $4 \cdot 10^{-3}$ M for the complex formed between gluconolactone and amyloglucosidase. The two values are in good agreement.

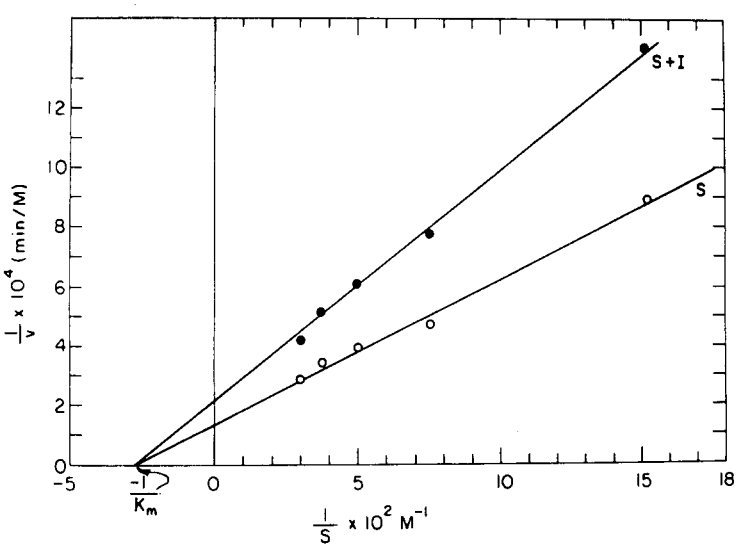

Fig. 5. Lineweaver-Burk plots for enzyme with substrate *p*-nitrophenyl-α-D-glucopyranoside, in the presence and absence of δ-gluconolactone. The assay mixture (2.5 ml) contained 10 μg/ml exo-1,4-glucosidase. The substrate concentration was varied in the range $0.66 \cdot 10^{-3}$—$3.3 \cdot 10^{-3}$ M, pH 4.2; 60°C. ○———○, without gluconolactone; ●———● in the presence of 0.05 M δ-gluconolactone.

Sodium dodecylsulfate-polyacrylamide gel electrophoresis and hydrodynamic studies

A number of studies in the literature present data concerning the molecular weight of this enzyme. Pazur and Kleppe [2] used sedimentation and diffusion coefficients to calculate a value of 97 000 for the enzyme from *A. niger* [2]. Pazur and Okada [32] found the molecular weight of the *R. delmar* enzyme to be 100 000. King [33] published a value of 50 000 for the amyloglucosidase from *Coniophora cerebella* and Ohga et al. [34] noted a value to 69 000 for the enzyme from *A. oryzae*.

Fig. 6 displays typical profiles of sodium dodecylsulfate-acrylamide gel electrophoresis runs of native and reduced carboxymethylated exo-1,4-glucosidase. For the native enzyme the molecular weights of the two major components were estimated to be 63 000 ± 3000 and 57 500 ± 2500, respectively. A faint doublet was also noted with molecular weights of 30 000 and 28 000, respectively, presumably representing half the parent molecular weights. When large quantities of protein were applied to the gels (>50 μg), two extremely faint bands of 16 000 molecular weight were observed, as well as material of molecular weight >100 000. Densitometric scans of these gels revealed that the total amount of material represented by all minor bands was 2—5% of the major components.

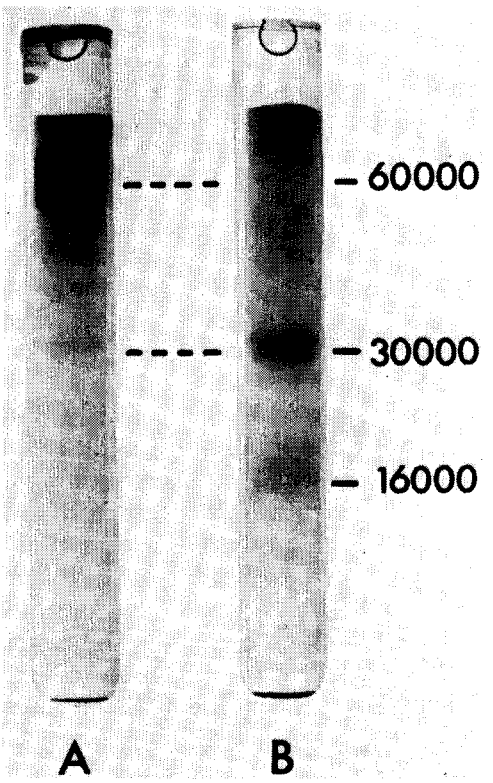

Fig. 6. Sodium dodecylsulfate-acrylamide gels of: A, native enzyme and B, reduced carboxymethylated enzyme. Each gel was loaded with approx. 30 μg of protein.

A sample of exo-1,4-glucosidase was reduced and carboxymethylated employing the forcing conditions outlined by Weber et al. [16], wherein the protein in 7–8 M guanidine · HCl, 100 mM β-mercaptoethanol, at pH 8.5 is heated in a boiling water bath for 5 min, incubated 2 h at 37°C and finally alkylated with iodoacetic acid. As can be seen in Fig. 6B, sodium dodecylsulfate-polyacrylamide gel electrophoresis of this material showed that the major species were the doublet with apparent molecular weights corresponding to 28 000–30 000. The 16 000 band was also considerably increased from that in the native enzyme. Densitometric scans indicated that these latter bands now made up approx. 40 and 20%, respectively, of the total protein, compared to <5% in the native case.

Multiple sedimentation and diffusion runs on the native material in either acetate buffer (0.1 M, pH 4.2) or Tris buffer (0.1 M, pH 7.0) over a concentration range of 1–8 mg/ml resulted in intrinsic $s_{20,w}$ and $D_{20,w}$ values of $5 \cdot 10^{-13}$ s and $6.35 \cdot 10^{-7}$ cm^2/s, respectively. At the relatively high Schlieren concentrations examined there was no indication that the samples underwent dissociation upon dilution. Further, the material sedimented and diffused as a single component in these runs, since the molecular kinetic properties of the two major bands observed in the sodium dodecylsulfate gels are indistinguishable, and the minor bands, representing smaller subunits of the protein, are present in amounts too small (<5%) to be detected in the Schlieren patterns. Substituting the intrinsic s and D values in the Svedberg equation, we obtain an apparent molecular weight of 62 200. For these calculations a partial specific volume of 0.70 ml/g has been used. This figure which is significantly lower than that used by Pazur and Kleppe [2] for the same calculation, has been calculated from the $\bar{v}$ values of the constituent protein and carbohydrate components by weight according to the relation:

$$\bar{v}_{enz} = \bar{v}_{pr} \cdot w_{pr} + \bar{v}_{cho} \cdot w_{cho}$$

where w_{pr} and w_{cho} are the weight concentrations of the protein and carbohydrate portions of the enzyme. $\bar{v}_{pr}$ and $\bar{v}_{cho}$ represent the $\bar{v}$ values of these same components as determined from literature values [35].

The intrinsic $D_{20,w}$ value was used for calculations of the frictional coefficient and axial ratio of the molecule using the tables of Svedberg and Pederson [28]. Substitution of the experimental value into the equation: $D = RT/fN$ (R = gas constant, f = frictional force per molecule), yields an f value of $61.4 \cdot 10^{-9}$. From Stokes' law and the molecular weight the frictional force on a perfect sphere of the same molecular weight (f_0) can be determined as $48.6 \cdot 10^{-9}$. The frictional coefficient, (f/f_0), for the enzyme therefore is 1.263, a value corresponding to an unhydrated prolate ellipsoid with an axial ratio of 5 : 1 [36]. Assuming an average degree of hydration of 0.2–0.3 g of water per g of protein, the value of f/f_0 would be reduced to the order of 1.1 implying that the hydrated protein particle is less asymmetric with an axial ratio of 3 : 1.

Sedimentation equilibrium data

Fig. 7 is a plot of weight average molecular weights versus protein concen-

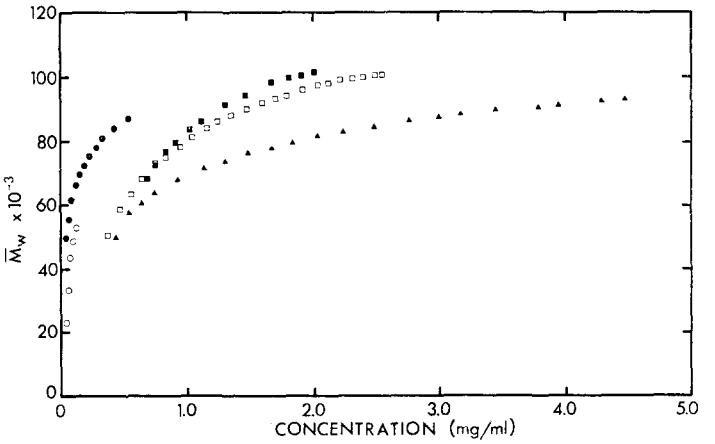

Fig. 7. Weight average molecular weight as a function of protein concentration in the cell for native enzyme. The results were obtained from several different initial protein loading concentrations: ▲, 1.83 mg/ml; □, 1.03 mg/ml; ■, 0.82 mg/ml; all at a rotor speed of 9000 rev./min. The data denoted by the symbolism: ●, 0.40 mg/ml and ○, 0.075 mg/ml were obtained at rotor speeds of 12 000 rev./min, respectively. Solvent system in all cases was 100 mM Tris · HCl at pH 8.0. Temperature was 20°C.

tration in the cell for several different initial loading concentrations at 9000 rev./min in a solvent system consisting of 100 mM Tris · HCl at pH 8. Inclusion of 1 mM dithiothreitol to this buffer did not seem to produce any significant alteration in the molecular weight distributions. Also included in this figure are data from two other runs employing the photoelectric scanner, one being measured at 280 nm and the other at much lower concentration, at 230 nm. The data in all cases apparently represent a protein system which undergoes dissociation upon dilution. The increase in the 28 000–30 000 bands on sodium dodecylsulfate-acrylamide gel electrophoresis after reduction and carboxymethylation of the native enzyme would perhaps suggest that the native molecule is a dimer, although the possibility of further dissociation to a 16 000 entity cannot be ruled out and hence a tetrameric structure is also feasible.

Optical rotatory dispersion studies

Optical rotatory dispersion curves were generated from 600 to 250 nm with the enzyme at pH values ranging from 4.2 to 9.0. The data presented in Fig. 8 were treated according to the Moffit and Yang technique [37], in which $[m']_\lambda [(\lambda^2 - \lambda_0^2)/\lambda_0^2]$ is plotted against $\lambda^2/(\lambda^2 - \lambda_0^2)$. The mean residue rotation was assumed to be 115 and the appropriate refractive index corrections have been made. It is apparent from the figure that linearization of data is only possible when λ_0 is taken as 205 nm rather than the usual 212 nm. The genesis of this conformational phenomenon is not apparent at the present time but the fact that a similar situation has been reported for fetuin [38], an acid glycoprotein of much the same size and sugar content, indicates that the interactions between the carbohydrate side chains and the peptide backbone may be responsible for the lower dispersion constant.

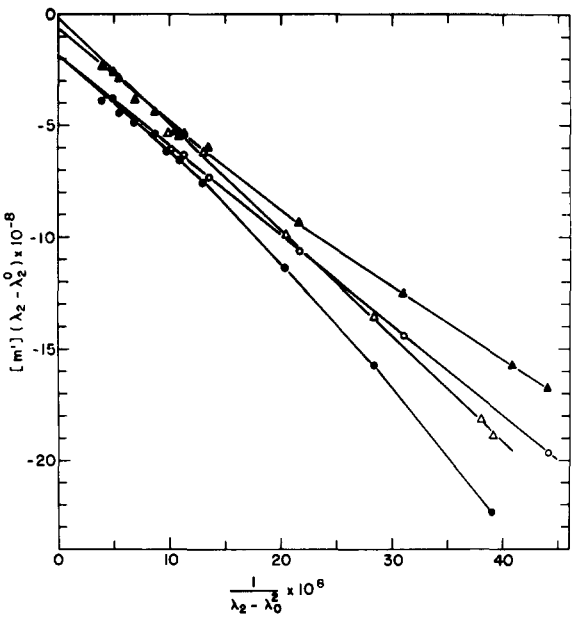

Fig. 8. Moffitt-Yang plots constructed for exo-1,4-glucosidase from visible ORD data. ○——○, λ_0 = 205 nm (acetate); △——△, λ_0 = 205 nm (phosphate); ●——●, λ_0 = 212 nm (acetate); ▲——▲, λ_0 = 212 nm (phosphate).

From the usual ordinate intercept and slope, an a_0 value of −2° and a b_0 value of −169° are obtained. From the latter figure an estimate of the apparent helical content of the enzyme can be made by comparison with similar data from synthetic polypeptides of known conformation. Assuming values for 100% α-helix and 100% random coil of −700 and 0°, respectively, upon linearizing Moffitt plots with a λ_0 of 205 nm [39], exo-1,4-glucosidase in its native configuration at pH 4.0 and 9.0 apparently contains 24% α-helix. Since the system shows dissociation below concentrations of 1 mg/ml, there is a possibility that the subunit optical activity may be somewhat different than that of the native enzyme [40].

The ORD spectrum of the molecule in the far ultraviolet region is reproduced in Fig. 9. The curve is not characteristic of the usual α-helical polypeptide since the minimum is seen between 228 and 230 nm rather than at 233 nm, while the cross-over point occurs at 221 nm. The position of a Cotton minimum at a wavelength lower than 233 nm, where the Cotton troughs for helical proteins are usually observed, has been found for other proteins as well [41]. In this case it may reflect the high carbohydrate content in amyloglucosidase which has been postulated to be the cause of a similar trough in fetuin [39].

Using the data of Greenfield et al. [42] and the $[m']_{230}$ value of −4000°, it could be calculated that amyloglucosidase contains 17% α-helix although the figure must be an overestimate due to contributions of both the antiparallel β form and the random chain to the rotation at this wavelength [43,44]. When the enzyme is heated to the temperature at which it is used commercially and at which the usual enzymatic assay is performed (60° C), the

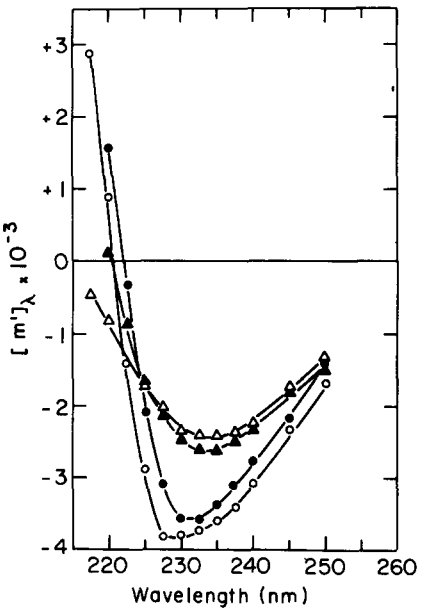

Fig. 9. Far ultraviolet ORD spectra of exo-1,4-glucosidase which had been preincubated at various temperatures for 15 min. ○— —○, 29° C; ●——● 48° C; ▲——▲, 57° C; △——△, 80° C.

ORD spectrum is altered as is also illustrated in Fig. 9. The magnitude of the major trough decreases minimally, the band width widens and in addition the maximum shifts toward the 233-nm value characteristic of the α-helix. Comparison of these curves with those published by several authors [42,45,46] leads us to conclude that exo-1,4-glucosidase is a mixture of the α, β and random forms and that the conformation shifts during temperature elevation from the ambient region to that of its maximal activity (60° C). It is also possible, of course, that the carbohydrate side chains of the molecule lead to interactions which result in the spectral shifts noted.

Circular dichroism studies

In order to clarify these observations, the circular dichroic spectrum of the native enzyme in the far ultraviolet region was recorded (Fig. 10). The negative portion of the curve is bimodal in character with ellipticity minima at 218 and 208 nm. Cross-over occurs at 201 nm and a positive peak of absolute ellipticity value 1.5 times that of the minima occurs at 193 nm. Comparison of these parameters with those published by others [45,47,48], reveals that the general shape of the experimental curves corresponds to that of the α-helical form of synthetic polypeptides rather than to the β or random conformations. Again, however, significant differences occur. The longest wavelength minimum is shifted 5 or 6 nm toward the blue and although cross-over is at the usually reported wavelength of 201 nm, the positive peak is also shifted 5 nm toward the blue. No direct evidence of a monotonic band at 217 characteristic of the β form is seen and the 198-nm minimum characteristic of random form in the far ultraviolet is also not evident. Using the data of Greenfield and Fasman [48],

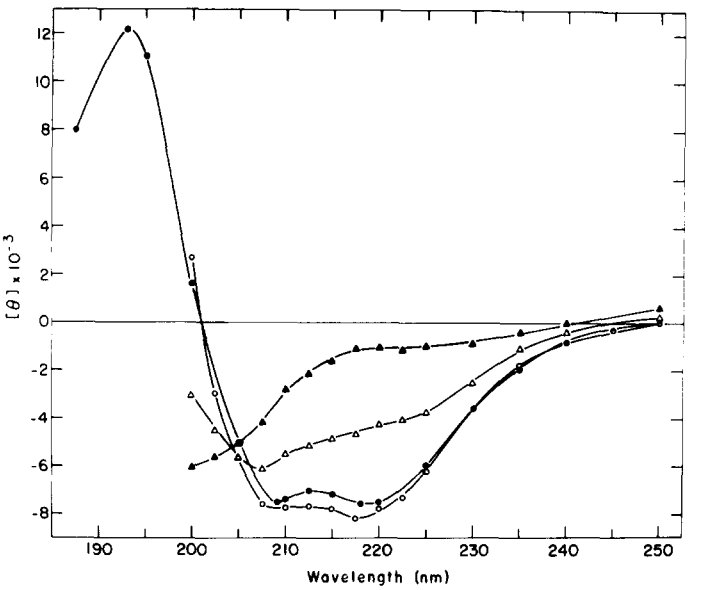

Fig. 10. Far ultraviolet CD spectra of exo-1,4-glucosidase at various pH values. ○——○, pH 7.0; ●——●, pH 9.4; △——△, pH 11.4; ▲——▲, pH 12.2.

an estimate of the amount of α-helix can be ascertained from the relationship:

$$\% \alpha\text{-helix} = \frac{[\theta]_{208\ nm} - 4000}{33000 - 4000}$$

and the enzyme can thus be estimated to contain 12% α-helix by this approximation. Although a great deal of significance should not be assigned to such an apparent α-helical value determined by ORD/CD, since the generated curves reflect other parameters such as the carbohydrate content of the protein, it appears certain that amyloglucosidase contains a small amount of α-helix, in the range of 15–20%

The explanation of the spectral abnormalities (the deviations from the typical α-helical curve) are not entirely clear but theoretically may be attributed to several phenomena. The blue shift of the major minimum in the 222–218 nm region has been found by Schellman and Lowe [49] in ribonuclease and has been attributed to short or badly distorted runs of helix in the molecule. In the same manner, the diminished magnitude of the major maximum at 193 nm can be attributed to a contribution from areas in random conformation since the characteristic CD spectrum of random polypeptides manifests an intense minimum at 197 nm. Superimposition of this minimum could also explain the shift of the maximum observed in this enzyme. Normally in the α-helix it occurs at 191 nm and in our data it is characteristically seen in the 193–195-nm region. It can be concluded from this portion of the study that the spectrum of exo-1,4-glucosidase, although appearing predominantly α-helical in character, must consist of contributions from all three forms.

Fig. 10 also displays spectra generated at alkaline pH values and it is apparent that the conformation of the molecule gradually shifts. The 218-nm

minimum remains as a shoulder at pH 11.5 and a shift to lower wavelengths occurs in the far ultraviolet minimum. The curve at pH 11.4 shows however, that the lower wavelength contribution attributed to the $\pi - \pi^*$ transition in the α-helix persists longer than does the minimum at 223 218 attributed to the $\eta - \pi^*$ transition [50]. Parallel studies of enzymatic activity indicate that it is in this same region, (pH 11.0—12.0), that activity of the enzyme is irreversibly lost. At pH 12.2 the CD curve is essentially that of the random configuration, although far ultraviolet absorption in the sample prohibited us from generating any inflections below 200 nm.

The fine structure of the enzyme has been investigated through studies of the CD spectrum in the 300 250-nm range, which are illustrated in Fig. 11. Although ellipticities in this region are several orders of magnitude lower than those in the far ultraviolet region, the enzyme does have a definable, reproducible pattern. Both positive and negative contributions are evident. The negative area at higher wavelengths is broad with at least three superimposed minima at 285, 276 and 272 nm. Cross-over occurs at 260 nm and the positive peak found at 257 nm is approximately one-third the magnitude of the negative band. The genesis of these various transitions was investigated in the studies illustrated in Figs 11 and 12.

As the pH of the sample is raised from 9.5 to 12.2 (Fig. 11) the aromatic spectrum undergoes three distinct changes: the magnitude of the negative troughs at 285, 276 and 272 nm decreases, the cross-over point shifts to longer wavelengths, and the positive peak moves first toward higher wavelengths with an even greater increase in ellipticity. Sakai et al. [51] have shown in a series of studies that the increase in ellipticity of stem bromelain in this same region

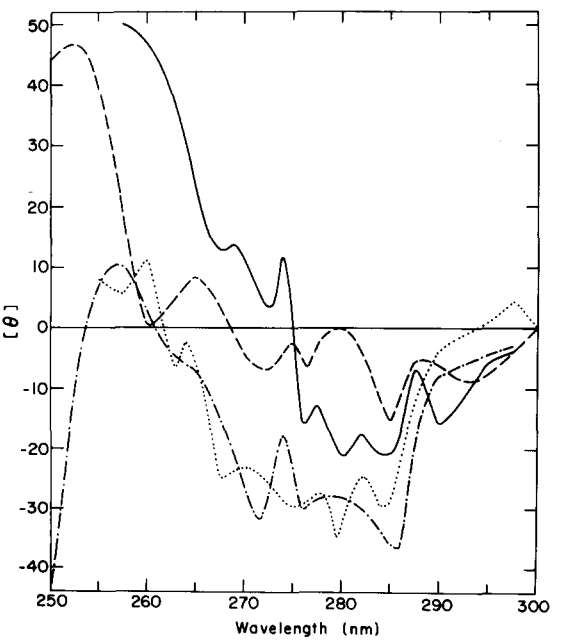

Fig. 11. Near ultraviolet CD spectra of exo-1,4-glucosidase at various pH values. •———•, pH 7.0; · · · · · ·, pH 9.4; - - - - - -, pH 11.4; ———, pH 12.2.

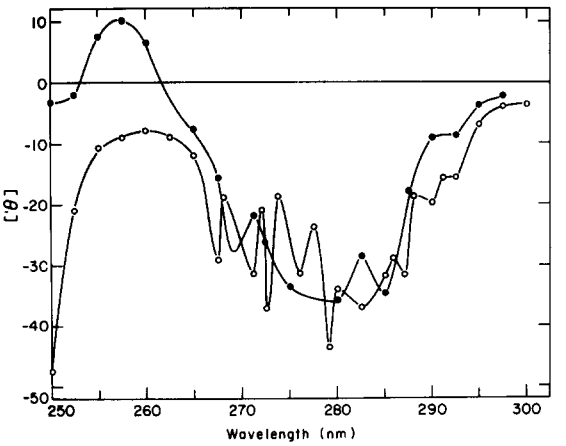

Fig. 12. Near ultraviolet CD spectra of modified exo-1,4-glucosidase. ●——●, O-acetylated; ○——○, reduced carboxymethylated.

parallels the ionization of tyrosine residues and Beychok [52] has concluded that, in lysozyme, alkaline shifts in this region are due both to tyrosine ionization and effects upon disulfide bridges. Since exo-1,4-glucosidase has 12 tyrosine residues and three disulfide bonds per molecule, both possibilities must be considered. CD studies on samples in which the tyrosine residues were modified by O-acetylation [23], as illustrated in Fig. 12, led to little overall change in the magnitude of the negative trough or the positive peak, although minor changes in the structure, exemplified by the appearance of a new negative trough at 279 nm, are apparent. Spectrophotometric titration, after Edelhoch [53], revealed that approximately one-third of the tyrosine residues were modified and in parallel 20% of the enzymatic activity was lost. Reduction and carboxymethylation [25], on the other hand, led to total loss of enzymatic activity, carboxymethylation of all six half-cysteine residues, and loss of the positive ellipticity band at 258 nm. Although other interpretations are possible since multiple alterations in the secondary and tertiary structure of the enzyme occur as the molecule unfolds, these data seem to indicate that the disulfide bonds in the native molecule contribute to the positive ellipticity band. Since the band underwent a red shift with increasing pH, a tyrosine contribution to this portion of the spectrum is also apparent [52]. The negative spectrum in the 272—285-nm region is probably due to both tyrosine and tryptophan contributions but it is not possible for us to sort these contributions out at the present time.

These same modified proteins were studied in the far ultraviolet region by circular dichroism and the results are presented in Fig. 13. O-Acetylation of one-third of the tyrosines leads to a minor decrease in the overall negative ellipticity but no change in the location of the major troughs at 218 and 208 nm occurred. The gross conformation of the molecule is, therefore, not affected. Reduction and carboxymethylation, however, changed the spectrum markedly so that all that remains is a shoulder at 224—226 nm and a negative trough characteristic of the disordered state at 205 nm. The latter pattern is similar to that seen following treatment of the enzyme in 5 M guanidine, the

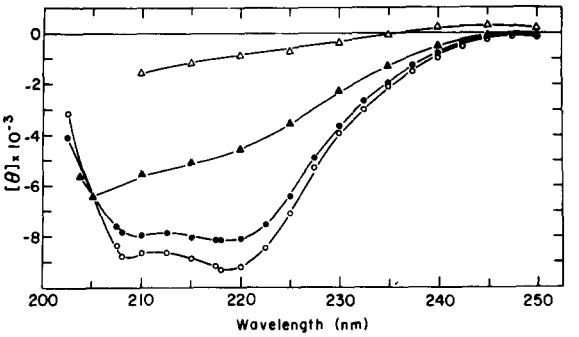

Fig. 13. Far ultraviolet CD spectra of modified exo-1,4-glucosidase. ○———○, control; ●———●, O-acetylated; ▲———▲, reduced carboxymethylated; △———△, guanidine treated.

results of which are also presented in the same figure. In both cases the ordered structure was largely destroyed and, in parallel, enzymatic activity was lost.

Spectropolarimeter data in presence of substrate and inhibitor

Since one of the overall aims of our studies of exo-1,4-glucosidase relates to definition of its active site, studies have been undertaken of the enzyme in the presence of its substrate as well as an effective inhibitor. The enzymatic reaction itself with either the synthetic substrate we have used (*p*-nitrophenyl-α-D-glucopyranoside) or its natural substrate, starch, are maximum at 60°C. For this reason before undertaking studies of the enzyme in the presence of substrate and inhibitor, we analyzed the changes in ORD and CD parameters following exposure to heat.

The ORD data presented in Fig. 9 and discussed previously indicate that the native configuration with a peak below 230 nm gradually shifts on elevation of the temperature so that the maximum deflection is seen at the wavelength more characteristic of α-helix-containing proteins, 233 nm. As the temperature is raised to even higher values the negative portion of the spectrum does not shift but the positive Cotton below 215 nm is decreased in magnitude. Fig. 14 demonstrates the time dependence of the conformational shift at 58° in ORD. Again, the movement of the negative Cotton toward the red is apparent during the 4-h period of this experiment. A CD study of this same phenomenon revealed that upon incubating the enzyme for 15 min at 60°C, the negative ellipticity bands of the native enzyme in the far ultraviolet are shifted several nm toward the red and overall loss in magnitude of the negative portion of the spectrum occurs. Our interpretation of these data is that with increasing temperatures some aggregation of the system is occurring which causes this red shift [54], and the reduction in negative ellipticity implies some melting out of the secondary structure with increasing temperature.

The far ultraviolet CD spectra of the enzyme in the presence of the substrate we have used for assay, and the inhibitor, 1,5-gluconolactone, are presented in Fig. 15. These data could only be obtained by the construction of difference curves since both the substrate and the inhibitor by themselves are optically active in the ultraviolet region. A further complication was introduced by the racemization of the inhibitor which occurs on heating and this phe-

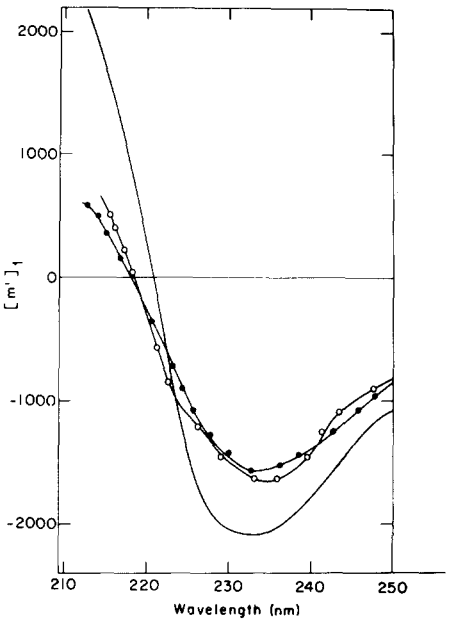

Fig. 14. Far ultraviolet ORD spectrum of exo-1,4-glucosidase heated at 58° C for various periods of time. ●——●, unheated; ○——○, 1 h; ●——●, 2 h.

nomenon is portrayed in Fig. 16. An equilibrium exists between the 1,5-form of the lactone, its 1,4 isomer and the parent gluconic acid and the approach to the equilibrium is reflected in a gross shift of the far ultraviolet ORD spectrum with time. Its presence introduced changes in the apparent CD pattern of the enzyme which had to be accounted for so that artefacts were not introduced in our interpretation.

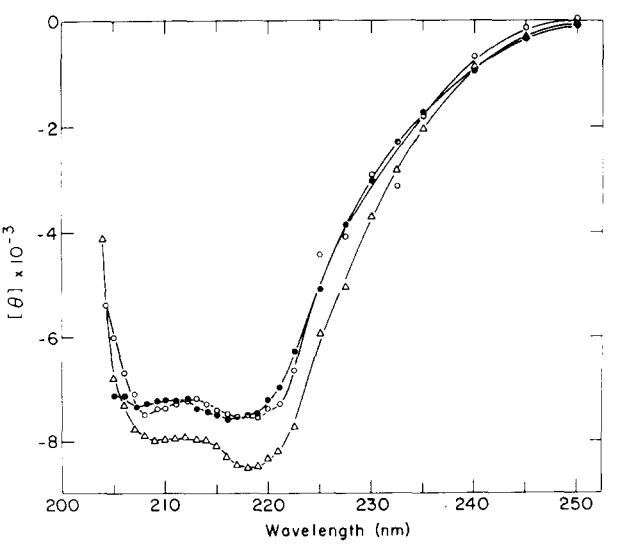

Fig. 15. Far ultraviolet CD spectrum of exo-1,4-glucosidase in the presence of inhibitor and/or substrate. △——△, enzyme control; ●——●, enzyme plus substrate ($3 \cdot 10^{-4}$ M); ○——○, enzyme plus inhibitor ($3 \cdot 10^{-3}$ M).

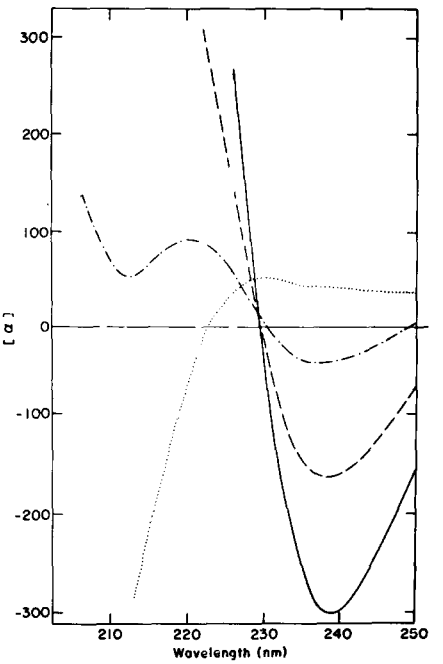

Fig. 16. ORD spectrum of 1,5-gluconolactone during incubation. ———, control; - - - - - -, 15 min; —·—·—, 30 min; · · · · · ·, 60 min.

The data in Fig. 15 indicate that a change in structure to a less ordered conformation occurs when the enzyme interacts with either its substrate or the inhibitor. Companion near ultraviolet CD data carried out but not shown in the CD spectra of amyloglucosidase from 300 to 190 nm in the presence of its substrate or inhibitor indicate that the conformation of amino acids involved in sites of optical asymmetry and their contribution to the aromatic spectrum are unaffected by the enzymatic reaction. Although multiple concentrations of substrate and inhibitor were evaluated, the data presented are those for the highest concentration we were able to study (optical activity of the material determining this limit). In the case of substrate this was the actual concentration used for routine studies of enzymatic activity and in the case of inhibitor it corresponded to 10^2 times the K_i (Levin, Y., Freedberg, I.M. and Katchalski-Katzir, E., unpublished).

Infrared spectroscopy

Since the CD and ORD data indicated the presence of α-helix, β form and disordered state in native exo-1,4-glucosidase the infrared studies displayed in Fig. 17 were undertaken. Spectra were obtained in ^2H_2O solution as well as from solid films made on NaCl plates. Comparison of these results with data summarized by Susi et al. [55] indicates that contributions from all three conformational states are in fact present. In ^2H_2O solution the peak at 1650 cm^{-1} characteristic of the α-helix, as well as the 1633 cm^{-1} contribution from the β form, and the broad band centered at 1642 cm^{-1}, attributed to the unordered state, are seen. On films, although peaks are less well resolved, the

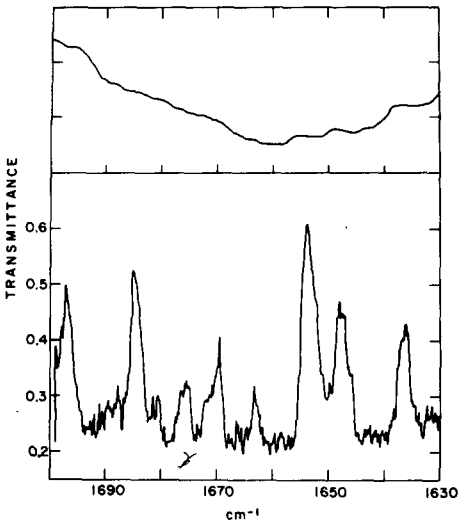

Fig. 17. Infrared spectra of exo-1,4-glucosidase. Details of preparative procedure as described in the text. Lower spectrum obtained in ^2H_2O solution: upper obtained from film.

1652-cm^{-1} α-helical contribution as well as the 1632-cm^{-1} contribution from the β form and the 1660-cm^{-1} band from the disordered state are apparent. In addition many other absorptive bands are present in both solution and on film. Some of the former are undoubtedly due to residual water absorption bands which occur in the same region as those identified as Amide I bands. In the latter case it is clear that this is not the case and further studies must be done to determine if non-peptide portions of the molecule, such as the carbohydrate residues, are responsible.

Acknowledgments

The authors are indebted to Mrs Gladys Traub for excellent technical assistance. Much of this work was carried out at the Weizmann Institute of Science where I.M. Freedberg was an American Cancer Society-American Contract Bridge League Faculty Research Associate and a Fellow of the John S. Guggenheim Foundation, and C.M. Kay held a Visiting Scientist Award of the Medical Research Council of Canada.

References

1 Pazur, J.H. and Ando, T. (1959) J. Biol. Chem. 234, 1966—1970
2 Pazur, J.H. and Kleppe, K. (1962) J. Biol. Chem. 235, 1002—1006
3 Pazur, J.H. and Ando, T. (1960) J. Biol. Chem. 235, 297—302
4 Fleming, I.D. and Stone, B.A. (1965) Biochem. J. 97, 13P
5 Lineback, D.R., Russell, I.J. and Rasmussen, C. (1969) Arch. Biochem. Biophys. 134, 539—553
6 Wilson, R.J.H. and Lilly, M.D. (1969) Biotechnol. Bioeng. Bioeng. 11, 349—362
7 Bachler, M.J., Strandberg, G.M. and Smiley, K.L. (1970) Biotechnol. Bioeng. 12, 85—92
8 Lowry, O.H., Rosebrough, N.J., Farr, A.L. and Randall, R.J. (1951) J. Biol. Chem. 193, 265—275
9 Bradstreet, R.B. (1965) The Kjeldahl Method for Organic Nitrogen, Academic Press, New York
10 Dubois, M., Gilles, K.A., Hamilton, J.K., Rebers, P.A. and Smith, F. (1956) Anal. Chem. 28, 350—356

11 Sternberg, M.Z. (1970) Biotechnol. Bioeng. 12, 1—17
12 Moore, S. and Stein, W.H. (1963) Methods in Enzymology (Kaplan, N.O. and Colwick, S.H., eds), Vol. 6, p. 819, Academic Press, New York
13 Davis, B.J. (1964) Ann. N.Y. Acad. Sci. 121, 404—427
14 Wrigley, C. (1968) Sci. Tools 15,17
15 Haglund, H. (1967) Sci. Tools 14,17
16 Weber, K., Pringle, J.R. and Osborn, M. (1972) Methods in Enzymology (Hirs, C.H.W. and Timasheff, S.N., eds), Vol. 26, pp. 3—27, Academic Press, New York
17 Ellman, G.L. (1959) Arch. Biochem. Biophys. 82, 70—77
18 Stark, R.G. and Smyth, D.G. (1963) J. Biol. Chem. 238, 214—226
19 Sanger, F. (1945) Biochem. J. 39, 507—515
20 Edman, P. (1956) Acta Chem. Scand. 10, 761—768
21 Hill, R.L. and Smith, E.L. (1957) J. Biol. Chem. 228, 577—599
22 Woods, K.R. and Wang, K.T. (1967) Biochim. Biophys. Acta 133, 369—370
23 Riordan, J.F., Wacker, W.E.C. and Vallee, B.L. (1965) Biochemistry 4, 1758—1765
24 Edelhoch, H. (1967) Biochemistry 6, 1948—1954
25 Crestfield, A.M., Moore, S. and Stein, W.H. (1963) J. Biol. Chem. 238, 622—627
26 Pickels, E.G. (1942) Chem. Rev. 30, 341—355
27 Fugita, H. (1962) Mathematical Theory of Sedimentation Analysis, Academic Press, New York
28 Svedberg, T. and Pederson, K.O. (1940) The Ultracentrifuge, Clarendon, Oxford
29 Chervenka, C.H. (1969) A Manual of Methods for the Analytical Ultracentrifuge, Spinco Division of Beckman Instruments, Inc., Palo Alto, California
30 Barton, L.L., Lineback, D.R. and Georg, C.E. (1969) J. Gen. Appl. Microbiol. 15, 327—344
31 Chipman, D.M., Grisaro, V. and Sharon, N. (1967) J. Biol. Chem. 242, 4388—4394
32 Pazur, J.H. and Okada, S. (1966) J. Biol. Chem. 241, 4146—4151
33 King, N.H. (1967) Biochem. J. 105, 577—583
34 Ohga, M., Shimizu, K. and Morita, Y. (1966) Agric. Biol. Chem. 30, 967—972
35 Gottschalk, A. and Graham, E.R.B. (1966) in The Basic Structure of Glycoproteins (Neurath, H., ed.), Vol. IV, The Proteins, Academic Press, New York
36 Schackman, H.K. (1959) Ultracentrifugation in Biochemistry, Academic Press, New York
37 Moffitt, W. and Yang, J.T. (1956) Proc. Natl. Acad. Sci. U.S. 42, 596—603
38 Green, W.A. and Kay, C.M. (1963) Arch. Biochem. Biophys. 102, 359—366
39 Verpoorte, J.A., Green, W.A. and Kay, C.M. (1965) J. Biol. Chem. 240, 1156—1161
40 Herskovits, T.T., Townsend, R. and Timasheff, S.N. (1964) J. Am. Chem. Soc. 86, 4445—4457
41 Jirgensons, B. (1969) Optical Rotatory Dispersion of Proteins and Other Macromolecules, Springer-Verlag, Berlin
42 Greenfield, N., Davidson, B. and Fasman, G.D. (1967) Biochemistry 6, 1630—1637
43 Davidson, B. and Fasman, G.D. (1967) Biochemistry 6, 1616—1629
44 Yang, J.T. (1965) Proc. Natl. Acad. Sci. U.S. 53, 438—445
45 Sakar, P.K. and Doty, P. (1966) Proc. Natl. Acad. Sci. U.S. 55, 981—989
46 Timasheff, S., Townsend, R. and Mescanti, L. (1966) J. Biol. Chem. 241, 1863—1870
47 Oikawa, K., Kay, C.M. and McCubbin, W.D. (1968) Biochim. Biophys. Acta 168, 164—167
48 Greenfield, N. and Fasman, G.D. (1969) Biochemistry 8, 4108—4115
49 Schellman, J.A. and Lowe, M.J. (1968) J. Am. Chem. Soc. 90, 1070—1093
50 Straus, J.H., Gordon, A.H. and Wallach, D.F.H. (1969) Eur. J. Biochem. 11, 201—212
51 Sakai, T., Ikeda, K., Hamaguchi, K. and Murachi, T. (1970) Biochemistry 9, 1939—1942
52 Beychok, S. (1965) Proc. Natl. Acad. Sci. U.S. 53, 999—1006
53 Edelhoch, H. (1967) Biochemistry 6, 1948—1954
54 Cassim, J.Y. and Yang, J.P. (1967) Biochem. Biophys. Res. Commun. 26, 58—64
55 Susi, H., Timasheff, S.H. and Stevens, L.J. (1967) J. Biol. Chem. 242, 5467